International Conference on Space Optics—ICSO 2014

La Caleta, Tenerife, Canary Islands

7–10 October 2014

Edited by Zoran Sodnik, Bruno Cugny, and Nikos Karafolas

Progress in diode-pumped alexandrite lasers as a new resource for future space lidar missions

M. J. Damzen

G. M. Thomas

A. Teppitaksak

A. Minassian

esa icso proceedings cnes

International Conference on Space Optics — ICSO 2014, edited by Zoran Sodnik, Nikos Karafolas, Bruno Cugny, Proc. of SPIE Vol. 10563, 1056339 · © 2014 ESA and CNES
CCC code: 0277-786X/17/$18 · doi: 10.1117/12.2304167

PROGRESS IN DIODE-PUMPED ALEXANDRITE LASERS AS A NEW RESOURCE FOR FUTURE SPACE LIDAR MISSIONS

M. J. Damzen[1], G.M. Thomas[1], A. Teppitaksak[1], A. Minassian[2]
[1]*The Blackett Laboratory, Imperial College London, U.K.* [2]*Unilase Ltd, London, U.K.*

I. INTRODUCTION:

Satellite-based remote sensing using laser-based lidar techniques provides a powerful tool for global 3-D mapping of atmospheric species (e.g. CO_2, ozone, clouds, aerosols), physical attributes of the atmosphere (e.g. temperature, wind speed), and spectral indicators of Earth features (e.g. vegetation, water). Such information provides a valuable source for weather prediction, understanding of climate change, atmospheric science and health of the Earth eco-system. Similarly, laser-based altimetry can provide high precision ground topography mapping and more complex 3-D mapping (e.g. canopy height profiling). The lidar technique requires use of cutting-edge laser technologies and engineered designs that are capable of enduring the space environment over the mission lifetime. The laser must operate with suitably high electrical-to-optical efficiency and risk reduction strategy adopted to mitigate against laser failure or excessive operational degradation of laser performance.

Laser sources with flexible wavelength and pulse capability would provide significant scientific and performance benefit to many remote sensing applications (e.g. resonant backscatter lidar, ground vegetation bio-mass/bio-health), however, there is a rather small set of laser technologies with suitable space-qualification or space heritage. Diode-pumped Nd:YAG lasers at 1064nm are established systems but offer no tunability, and even with their harmonics (532nm/355nm) entirely miss whole wavelength regions. Optical parametric conversion can be used but leads to higher complexity, reduction in reliability and considerable loss of efficiency. Vibronic solid-state lasers could provide an alternative approach due to their broad tunability and extended pulse capabilities. However, the most widely used vibronic scientific system, Ti-sapphire (Ti:S), usually requires complex pump sources, typically frequency-doubled Nd:YAG/Nd:YVO_4 lasers, that leads to high complexity and poor overall system efficiency. Attempts at CW blue diode-pumped operation of Ti:S has been very limited in power and efficiency [3,4] and prospects for Q-switched pulsed development are unattractive due to its very short upper-state lifetime ~3μs [1].

An alternative vibronic laser is Alexandrite (Cr-doped chrysoberyl). This laser occupies the spectral band ~700–858nm [5–8], which is particularly interesting for high sensitivity monitoring of bio-mass/bio-health as it overlaps the red-edge of chlorophyll, the steep rising transition region between high red absorption and high near–IR reflection. A key advantage of Alexandrite is its capability for direct pumping by red (AlGaInP) laser diodes with high absorption coefficient (~6cm^{-1} at 639nm, as shown in Fig.1) and small quantum defect leading to high efficiency potential and low heat dissipation. Its long upper-state (room-temperature) lifetime ~260μs [8] allows for good energy storage potential for Q-switched operation. Alongside these favourable diode pumping characteristics, Alexandrite has a number of superior thermo-mechanical properties for high power/energy operation: thermal conductivity (23$Wm^{-1}K^{-1}$) [8] is almost twice that of Nd:YAG; fracture resistance is five-times that of Nd:YAG [5]; and its strong birefringence gives highly linearly-polarised laser emission, eliminating depolarisation problems. The stimulated emission cross-section for Alexandrite is low (0.7x$10^{-20}cm^2$) requiring high laser fluence, but is offset by Alexandrite's extraordinarily high optical damage threshold (>270Jcm^{-2}) [8].

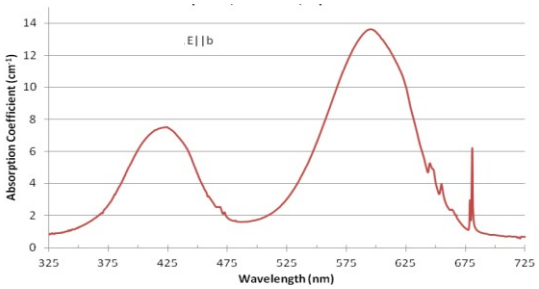

Fig. 1. Absorption spectrum for Alexandrite.

Despite its potential as a directly diode-pumped laser source to address high power, tunable and pulsed applications in this key wavelength region, there have been only a small number of publications reporting diode-pumped Alexandrite laser operation, the majority of which operating at very modest sub-Watt power level [10-

13] using diode end-pumping. Our previous work produced the first multi-Watt operation (6.4W) using a diode side-pumped Alexandrite slab laser approach [14].

In this paper we show some breakthrough results in the development of the diode-pumped Alexandrite laser technology. We experimentally demonstrate multi-ten-Watt (26.2W) powers with high slope efficiency (49%) in an end-pumped rod laser configuration. This power is one to two orders of magnitude higher than previous diode end-pumped demonstrations and the highest slope efficiency of diode-pumped Alexandrite lasers to date. High power side-pumped slab Alexandrite operation in the grazing incidence bounce amplifier geometry is also demonstrated for the first time in this laser crystal. The latter part of this paper provides details of a prototype laser design we have configured towards a remote sensing performance with TEM_{00} cavity design, high repetition rate electro-optic Q-switched operation and wavelength tuning using a self-seeding technique. This is the first Q-switched operation of a diode-pumped Alexandrite laser, to our knowledge. Preliminary results show ~mJ-level pulse energy at 1kHz pulse rate in fundamental TEM_{00} operation.

II. COMPACT END-PUMPED ROD AND SIDE-PUMPED SLAB LASER CONFIGURATIONS:

To understand the performance of high power diode pumping with low brightness red diode bars we performed initial studies using compact laser cavities to discern the power scaling and efficiency potential of the Alexandrite. Two configurations were employed: an end-pumped rod laser cavity (Fig. 2a) and a side-pumped slab laser employing a grazing incidence bounce geometry of the laser mode from the pump face (Fig. 2b).

The end-pumped Alexandrite laser rod configuration is shown in Fig. 2a. The laser had a compact plane-plane mirror cavity with cavity length 15mm. The back mirror (BM) was highly-reflecting (R>99.9%) at laser wavelength (~755nm) and highly-transmitting (R<0.2%) for pump diode laser (~639nm). Several output couplers (OC) were tested with reflectivity R_{OC}. Two Alexandrite rods were investigated in this work, both with length 10mm and diameter 4mm: one with 0.13 at.% and the other with 0.22 at.% Cr-doping. The end faces of the rods were plane-parallel and anti-reflection coated at the Alexandrite wavelength (~755nm). Both rods were mounted in water-cooled copper heat-sinks. The absorption coefficient for the two crystals (measured @633nm), was ~4cm^{-1} for the 0.13 at.% rod and ~6cm^{-1} for the 0.22 at.% rod. Pumping was achieved with a red diode module, operating nominally at 639nm with bandwidth (FWHM) of 1.2nm and capable of providing high pump power exceeding 60W in continuous-wave mode. The highly-multimode spatial output of this module (fast axis M_f^2 ~25; slow axis M_s^2 ~200) was reshaped with cylindrical lenses, providing a near-circularised pump beam with spot size (FWHM) ~350µm located near the input face of the rod. The polarisation of the module was near-linear (with polarisation purity ~95%) in the fast axis and was oriented parallel to the *b*-axis of the Alexandrite rod for maximum absorption.

The side-pumped slab laser using a bounce amplifier geometry design is shown in Fig. 2b. In this geometry, the laser mode makes a total internal reflection (bounce) from the pump face of the Alexandrite amplifier providing the laser mode with good access to the high inversion at that face, aiding high efficiency and giving a considerable averaging across the inhomogeneous thermal and gain distribution in the depth of the crystal, enhancing the potential quality of the TEM_{00} mode. The Alexandrite slab had dimensions: 20 x 4 x 2 mm and doping 0.235 % Cr. The slab was side pumped by an identical red diode pump as the end-pumped system with diode polarized parallel to crystal *b*-axis and focused using a single vertical cylindrical lens (f=80mm) to form a horizontal line focus on the pump face (20 x 2mm) with dimensions ~ 12mm x 100µm. The cavity mode operated with 9^0 internal bounce angle to pump face and cavity length was ~ 40mm. Back mirror was plane and high reflecting (HR) at 755nm, output coupling mirror was plane with reflectivity R_{OC}=98%.

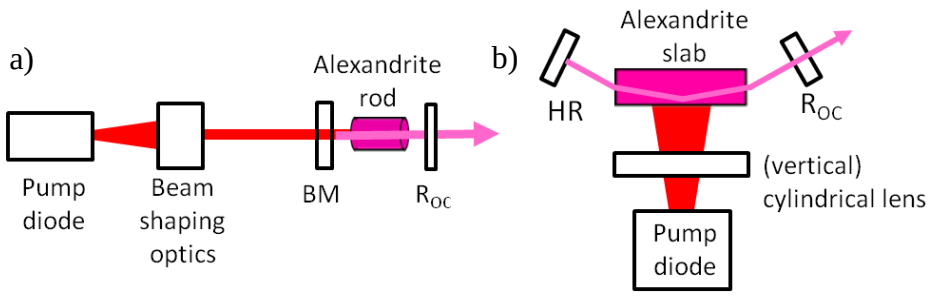

Fig. 2. Schematic diagrams of compact Alexandrite laser configurations: a) End-pumped rod laser (BM=back mirror (HR755nm/HT639nm)); b) Side-pumped Alexandrite slab laser in bounce geometry cavity configuration. Output coupler with reflectivity R_{OC}.

A. Performance data of the compact end-pumped Alexandrite rod laser

Fig. 3 shows the results of the output power of the diode end-pumped laser against absorbed pump power, using the 0.13 at.% rod with the output coupler (OC) of reflectivity R=99%.

The results for pumping with the near-circularised pump diameter (FWHM) ~350μm (red circles) show an output power of 21.3W with 57.8W of absorbed pump power, corresponding to an optical-to-optical conversion efficiency of 37%. The slope efficiency is 41%. The fast-axis size of the pump beam was decreased to ~210μm, whilst maintaining the slow-axis size (~350μm), to demonstrate the effect of more intensive pumping. The results of this are also shown (blue squares) in Fig. 3. The slope efficiency of the laser increased to 45%, and an output power 26.1W was produced for absorbed pump power of 64.5W (optical-to-optical efficiency 40.5%).

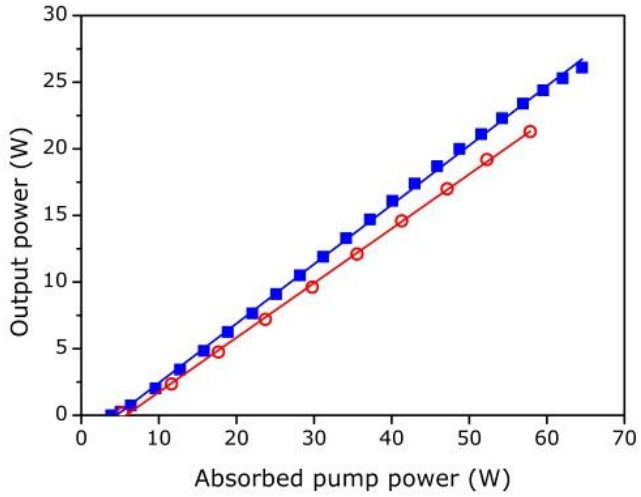

Fig. 3. Output power against pump power for Alexandrite laser, rod doping 0.13 at.%; output coupler R_{OC}= 99%. Red circles are data for circular-pump diameter ~350μm; blue squares are data for reduced fast-axis pump size ~210μm. Lines are linear fits to the power curves.

Fig. 4 shows the peak lasing wavelength and lasing bandwidth (FWHM) against pump power for the circularised pump beam of ~350μm diameter. The laser shifts to longer wavelengths with increasing pump power, which may be associated with increasing crystal temperature [6]. The wavelength near 60W pumping is ~759nm. The lasing bandwidth narrows from about 4 nm at 20W pumping to 2.3 nm near 60W.

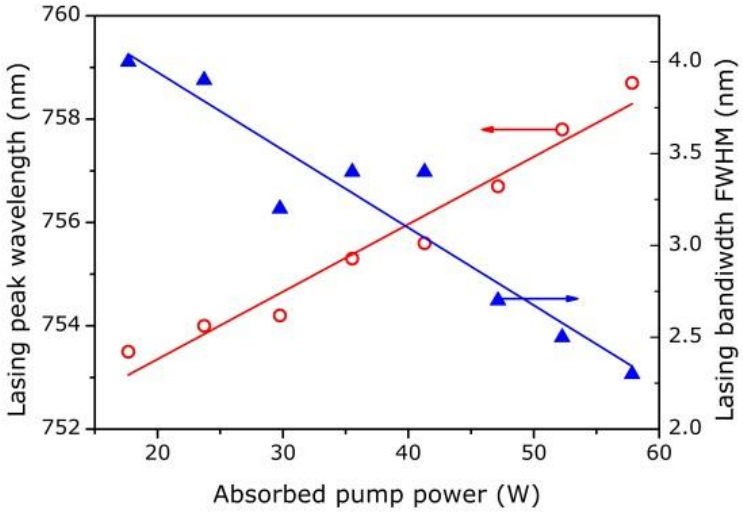

Fig. 4. Lasing peak wavelength and lasing bandwidth against pump power for diode end-pumped Alexandrite laser with circularised pump beam diameter ~350μm (0.13 at.% rod).

Figure 5 shows the output power for the end-pumped Alexandrite laser, this time using the higher doped 0.22 at.% rod, for OC reflectivity R_{OC} from 99% to 95%. The highest slope efficiency was 49% for the R_{OC}=99% output coupler with the reduced pump size (fast-axis size ~210μm) producing 26.2W at the pump level of 64.5W. It is noted that the slope efficiency at lower pumping level is even higher than 49%. Threshold is somewhat higher and there is more evidence of roll-over at high pump power than the 0.13 at.% rod, although some of this effect may be cavity alignment. The variation of output power with different R_{OC} using the 350μm circular pump size reveals a trend to lower slope efficiency with lower OC reflectivities: 43% (R_{OC}=99%); 39% (R_{OC}=98%); 33% (R_{OC}=97%); and 31% (R_{OC}=95%). The decreased slope efficiency is not consistent with simple 4-level laser theory, and has been noted previously [15]. It may suggest the presence of energy transfer up-conversion in the Alexandrite crystal and would be worthy of further investigation.

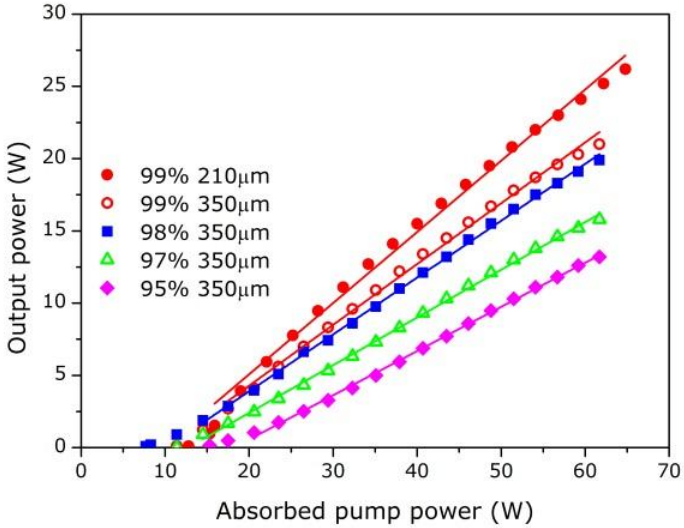

Fig. 5. Output power against pump power for Alexandrite laser, rod doping 0.22 at.%, for different output coupler reflectivity. Lines are linear fits to the power curves.

The results for the two Alexandrite rod lasers show that the output power is limited only by the pump power. Just two pump distributions were attempted in this study and it is likely that with further pump optimisation even higher efficiency can be achieved. It is informative to consider some efficiency factors involved in the Alexandrite laser. The photon quantum efficiency (ratio of laser to pump photon energy) = λ_p/λ_L = 84% where λ_p and λ_L are the pump and laser wavelength, respectively. The cavity loss factor = T/(T+L) ~ 71%, where T=1% is the output coupling transmission and L ~0.4% is the roundtrip intracavity loss (due to the rod AR-coatings). The beam overlap efficiency (fill-factor) between the laser mode volume with the gain volume is estimated to be ~80–90% [16]. The pump quantum yield is taken to be 100% [5]. The product of these efficiency factors gives slope efficiency ~48–54%. Interestingly, Scheps [11] achieved 63.8% slope efficiency of an Alexandrite laser pumped by a red dye laser at 645nm, and this demonstrates that higher efficiency is possible with better optimised cavity and diode pumping.

B. Performance data of the compact side-pumped bounce geometry Alexandrite slab laser

The bounce laser cavity was run with CW diode pumping. The laser output power as function of diode pump power is shown in Fig. 6 as well as a photograph showing the fluorescence from the top of the slab crystal. The output power was 10.2 W (at ~ 755nm) for incident pump power of 67W. This is an optical-to optical conversion of 21% and slope efficiency is ~ 23% (or with respect to absorbed pump optical-to-optical efficiency of 25% and slope efficiency ~ 28%).

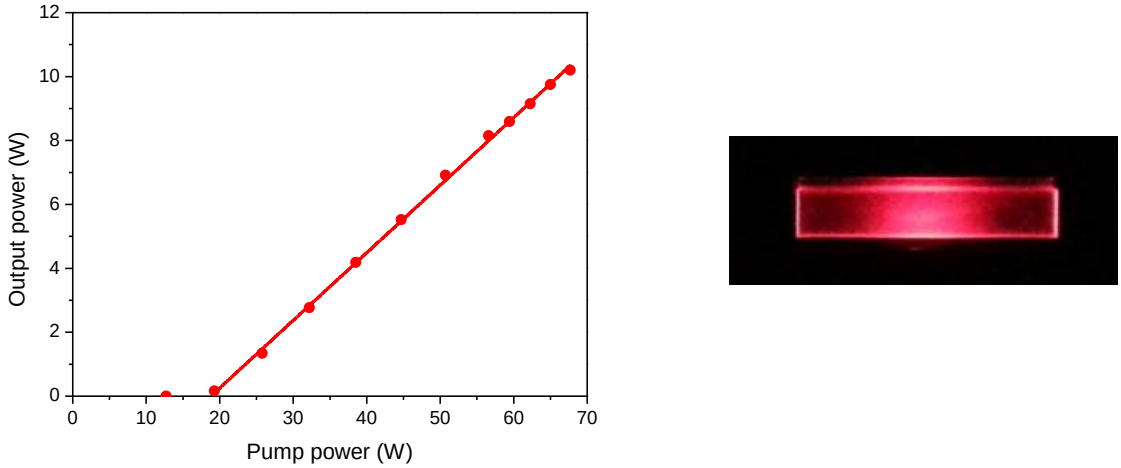

Fig. 6. Side-pumped Alexandrite slab laser: a) output power in bounce geometry cavity configuration, and b) photograph of the fluorescing crystal taken from the top of the slab.

In the above experiment the diode pump was run with water cooling at 20°C. The efficiency was found to increase by running the pump diodes at lower temperature as shown in Fig. 7 showing the output power as a function of pump diode water temperature. The laser power is 10.2 W at 20°C but increases to 12W at 12°C, and decreases in power at higher than 20^0C temperature. The power increase with decreasing temperature of diode water temperature is shown to correlate to pump wavelength which tunes to shorter wavelength (also shown on Fig. 7). At shorter wavelength the pump absorption increases (absorption depth decreases). This enhances the inversion density at the pump face and gain experienced by the laser mode as well as the extraction efficiency at the pump face in the bounce geometry. It is also noted that the laser mode experiences considerable reflection losses at the two slab crystal faces since the laser mode is far from normal incidence where the AR coatings are designed for. In addition to the 12 W power measured from the output coupling mirror at 12^0C, there is > 2W power ejected from the slab face reflections. If the coatings are optimised for the angle of incidence to these faces (or the faces angled appropriately) for the desired bounce angle, further power efficiency would be achieved. Additional advantage would come from using even higher Cr-doping, producing the same power improvement due to higher pump absorption coefficient as with temperature tuning of the diode laser: increasing the gain volume overlap to the laser mode as well as enhanced gain experienced by the more intensive pumping.

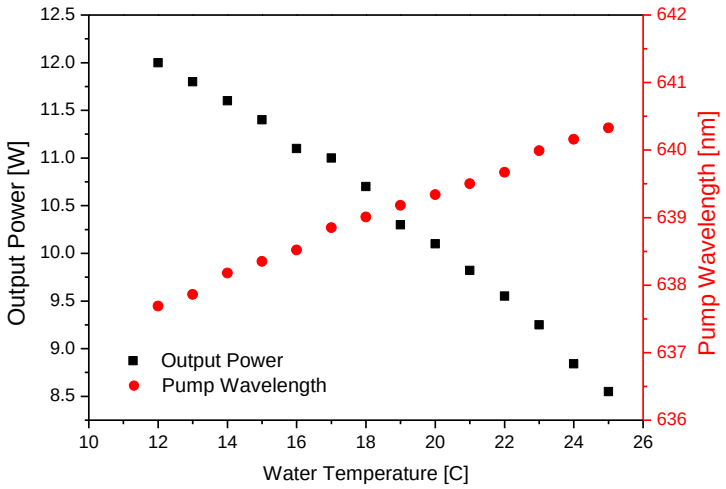

Fig. 7. Output power of the Alexandrite slab laser in bounce geometry cavity as function of pump diode water temperature. Pump wavelength is also shown in red.

III. PROTOTYPE Q-SWITCHED/WAVELENGTH-TUNED TEM_{00} END-PUMPED LASER DESIGN:

This section describes a first attempt at configuring the Alexandrite laser for tunable, Q-switched and TEM_{00} operation. A motivation for developing such a pulsed laser source is to address space-borne remote sensing applications, including atmospheric lidar and altimetry.

Fig. 8 shows an extended end-pumped laser cavity design (cavity length ~125mm), with intracavity plano-convex lens (PCX, f=100mm) and Pockels cell Q-switch. The intra-cavity lens design was chosen to optimise for TEM_{00} operation and also to achieve a larger mode size in the resonator near sensitive optics, e.g. to minimise laser-induced damage to the Pockels cell. The OC with lower reflectivity (R_{OC}=95%) was chosen to reduce the intra-cavity flux, that also may cause laser-induced damage especially under high peak power Q-switched operation. For this part of the study, the laser rod with 0.22 at.% Cr-doping was used with circularised pump size ~350μm. An external feedback grating was used, just for the wavelength tuning demonstration.

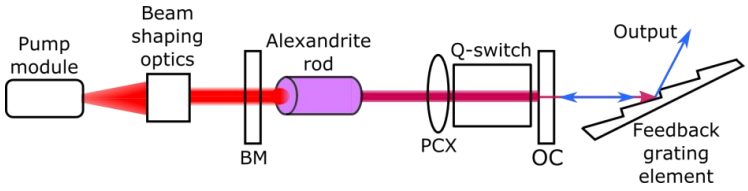

Fig. 8. Alexandrite TEM_{00} laser design for Q-switching and wavelength tuning.

A. Wavelength-tuning demonstration

A brief investigation was undertaken to explore the impact of wavelength tuning on the performance of the end-pumped laser. A 1800 lines mm^{-1} holographic grating was placed external to the output of the laser cavity, in Littrow configuration, as shown in Fig. 8. Tuning of the cavity was achieved by adjusting the angle of the grating, with the first diffraction order providing the seed to the cavity, and the zeroth order used as the output. The laser was tuned continuously between 730–792nm, with cavity in free-running (non-Q-switched) mode. Outside of this range, the cavity reverted to the central wavelength of Alexandrite, ~755nm. Tuning was limited by self-seeding strength but indicative that a much broader tuning range is possible. It is noted that at 792nm, the output power was 39% of the power at peak wavelength ~755nm.

B. Q-switching results

For Q-switching demonstration, the pump module was operated in quasi-continuous wave (QCW) mode with adjustable pump duration and repetition rate, as required. The Q-switching element was a BBO Pockels cell. The Pockels cell was operated at 2kV, near its quarter-wave voltage with the voltage applied during diode pumping to inhibit lasing, and the voltage then removed at the end of the pump pulse to induce Q-switched output. To minimise complexity, Q-switched operation was achieved without intracavity polariser or Brewster plate. The loss modulation was based on a polarisation switching technique [5,15] where the Pockels cell achieves loss by switching the laser polarisation to the lower gain axis of Alexandrite on alternate cavity transits. This requires no additional Brewster plate or polariser, but the Pockels cell hold-off, in principle, is limited to twice threshold pumping of the cavity [15].

Figure 9 shows Q-switched output energy against pump energy, for two example cases. In case 1 (red squares), the laser cavity length was 125mm; the intra-cavity lens had focal length 100mm and was positioned to form a stable cavity configuration and to optimise TEM_{00} operation. Pulse energy 0.74mJ (pulse duration 92ns) was achieved at 1kHz repetition rate for a pump duration of 0.22ms, for circularised pump size ~350μm. In case 2 (blue circles), a shorter cavity of length 60mm was used, without the lens, with pump duration 0.2ms and fast-axis pump size reduced to 210μm. Pulse energy 0.7mJ (pulse duration 58ns) was achieved at 100Hz; the slope efficiency is 12.5%. Beam quality was TEM_{00} with M^2 ~1.1 for all cases, except the final point for 1kHz pulse data (M^2 ~1.6) where the mode size was adjusted to achieve higher output energy by increased mode-gain overlap. Higher pulse energy scaling was limited by Pockels cell hold-off.

The pulse energy and efficiency of the laser increased, in general, with repetition rate. The improvement is thought to be due to the increasing pump heat loading and hence higher temperature of the crystal that enhances its emission cross-section [6].

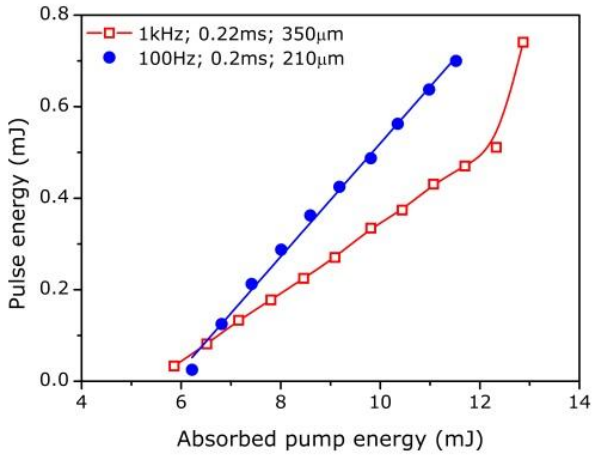

Fig. 9. Output pulse energy against pump energy for TEM_{00} Q-switched Alexandrite laser. Red squares at 1kHz pulse rate (pump duration 0.22ms; pump size 350μm); blue circles at 100Hz (pump duration 0.2ms; pump fast-axis size 210μm).

IV. CONCLUSIONS:

We show for the first time that highly efficient, multi-ten Watt operation of an Alexandrite laser can be achieved with direct high-power red diode-pumping, even with relatively low brightness diodes. A diode end-pumped Alexandrite rod laser has demonstrated output power 26.2W, more than an order of magnitude higher than previous diode end-pumped Alexandrite lasers. A slope efficiency of 49% was demonstrated, the highest reported for a diode-pumped Alexandrite laser to date. In a diode-side-pumped Alexandrite slab in the bounce geometry 12W of output power was achieved, and it was shown that much higher efficiency should be possible with enhanced pump absorption to increase gain volume extraction, and by elimination of surface losses.

A prototype end-pumped Alexandrite laser has been developed and tested for Q-switched TEM_{00} operation and an initial assessment of wavelength tuning made. Wavelength tuning between 730–792 nm was demonstrated, with a self-seeding technique using feedback from an external grating. Much wider tuning range is expected with improved feedback control. Q-switched laser operation based on a polarisation switching technique shows initial results with ~mJ-pulse energy at kHz pulse rate in TEM_{00} operation. It should be stated that this laser system is unoptimised and there is considerable scope for performance improvements, including higher temperature operation of Alexandrite where the effective emission cross-section can be increased [5], and enhanced cavity design with optimised pumping. Alongside the end-pumped design, the side-pumped slab Alexandrite laser can be developed for a more scalable route to higher powers and higher pulse energy capability.

This work shows exciting prospects for the development of Alexandrite as a directly-diode pumped solid-state laser source. It can address remote sensing applications in the ~ 700-850 nm wavelength region as a more efficient, compact and simple laser approach compared to OPO conversion of a frequency-doubled Nd:YAG laser source. This wavelength region is particularly interesting as it overlaps the spectrally-sensitive Red-Edge of vegetation providing a higher precision index (e.g. Red-Edge NDVI) of vegetation content and stress [17]. With second harmonic generation, Alexandrite also operates as a tunable UV laser source, again offering simplification and efficiency advantage over Nd:YAG where frequency-tripling is required. The tunability of UV Alexandrite can provide spectrally optimized backscatter lidar (e.g. resonant backscatter) and by operating at somewhat longer UV wavelengths (e.g. 380nm) compared to 355nm operation from Nd:YAG offers prospects for reducing UV degradation of optics in the laser transmitter system.

V. ACKNOWLEDGMENTS:

We gratefully acknowledge financial support for this work from the European Space Agency (ESA) under contract 4000107239/12/NL/PA.

REFERENCES

[1] P. F. Moulton, "Spectroscopic and laser characteristics of Ti:Al_2O_3," J. Opt. Soc. B. **3**, 125-133 (1986).
[2] D. E. Spence, P. N. Kean, and W. Sibbett, "60-fsec pulse generation from a self-mode-locked Ti:sapphire laser," Opt. Letters **16**, 42-44 (1991) .
[3] P. W. Roth, A. J. Maclean, D. Burns, and A. J. Kemp, "Directly diode-laser-pumped Ti:sapphire laser," Opt. Letters **21**, 3334-3336 (2009).
[4] P. W. Roth, D. Burns, A. J. Kemp, "Power scaling of a directly diode-laser-pumped Ti:sapphire laser," Opt. Exp. **20**, 20629-20634 (2012).
[5] J. Walling, O.G.Peterson, H. Jenssen, R. Morris, and E. W. O'Dell, "Tunable Alexandrite lasers," IEEE J. Quant. Elec. **16**, 1302-1315 (1980).
[6] J. W. Kuper, T. Chin, and H. E. Aschoff, "Extended tuning range of Alexandrite at elevated temperatures," Proc. Advanced Solid State Lasers (OSA) **6**, paper CL3 (1990).
[7] R. C. Powell, L. Xi, X. Gang, G. J. Quarles, and J. C. Walling, "Spectroscopic properties of alexandrite crystals," Phys. Rev. B **32**, 2788-2797 (1985).
[8] J. Walling, D. F. Heller, H. Samelson, D. J. Harter, J. Pete, and R. C. Morris, "Tunable alexandrite lasers: Development and performance," IEEE J. Quant. Elec. IEEE J. Quant. Elec. **21**, 1568-1581 (1985).
[9] U. Demirbas, M. Schmalz, B. Sumpf, G. Erbert, G. S. Petrich, L. A. Kolodziejski, J. G. Fujimoto, F. X. Kaertner, and A. Leitenstorfer, "Femtosecond Cr:LiSAF and Cr:LiCAF lasers pumped by tapered diode lasers," Opt. Exp. **19**, 20444-20460 (2011).
[10] R. Scheps, B.M. Gately, J.F. Myers, J.S. Krasinski, and D. F. Heller, "Alexandrite laser pumped by semiconductor lasers," Appl. Phys. Letters **56**, 2288-2290 (1990).
[11] R. Scheps, J. F. Myers, T. R. Glesne, and H. B. Serreze, "Monochromatic end-pumped operation of an Alexandrite laser," Opt. Comm. **97**, 363-366 (1993).
[12] X. Peng, A. Marrakchi, J. C. Walling and D. F. Heller, "Watt-level red and UV output from a CW diode array-pumped tunable Alexandrite laser," in Conference on Lasers and Electro-Optics. Paper CMAA5, OSA (2005).
[13] E. Beyatli, I. Baali, B. Sumpf, G. Erbert, A. Leitenstorfer, A. Sennaroglu, and U. Demirbas, "Tapered diode-pumped continuous-wave alexandrite laser," J. Opt. Soc. Am. B **30**, 3184-3192 (2013)
[14] M. J. Damzen, G. M. Thomas and A. Minassian, "Multi-watt diode-pumped alexandrite laser operation," in CLEO Europe, Paper CA-2.6 SUN (2013).
[15] C.J. Lee, P.J.M van der Slot and K-J. Boller, "A gain-coefficient switched Alexandrite laser," J.Phys.D: Appl. Phys. **46**, 015103 (2013).
[16] W. Koechner and M. Bass, *Solid-State Lasers: A Graduate Text* (Springer-Verlag, New York, 2003).
[17] J.U.H. Eitel et al, "Broadband, red-edge information from satellites improves early stress detection in a New Mexico conifer woodland", Remote Sensing of the Environment **115**, 3640-3646 (2011).